

Influence of Geometry on the Hall Effect in Ballistic Wires

C. J. B. Ford, S. Washburn, M. Büttiker, C. M. Knoedler, and J. M. Hong

IBM Thomas J. Watson Research Center, P.O. Box 218, Yorktown Heights, New York 10598

(Received 3 March 1989)

We present a systematic investigation of the influence of cross geometry on the Hall effect in narrow ballistic wires. Various differently shaped cross regions have been fabricated, which demonstrate that near zero magnetic field the Hall resistance can be quenched, enhanced over its classical value, or even *negative*. A “last plateau” is seen in all devices, proving that its cause is not intimately linked to the quenching. A simple physical picture is presented showing how these effects come about from the scattering of electrons in such geometries.

PACS numbers: 72.20.My, 73.50.Jt, 73.60.Br

The quenching of the Hall effect is an intriguing result observed in narrow high-mobility devices by Roukes *et al.*¹ and others.^{2,3} As the magnetic field B is reduced, the Hall resistance R_H (measured at voltage probes on either side of a narrow channel) forms a plateaulike feature (the “last plateau”) and then drops sharply below its classical value so as to be close to zero (“quenched”) in some finite region around $B=0$. This phenomenon has received considerable theoretical attention but it still lacks a definitive explanation. It has not been clear whether or not the last plateau and the quench are related, or indeed whether the effects are explicable solely in terms of single-particle transport theory. In this Letter, we describe measurements on several different cross geometries which yield alternatively quenched, enhanced, or negative R_H . The last plateau, however, appears in all samples.

It has been proposed that R_H would be quenched if the channel width were less than the size of the edge states formed by the Lorentz force,⁴ but the quantitative agreement with experiment was limited.² Very recently such narrow channels have been modeled quantum mechanically by a direct numerical solution of the Schrödinger equation together with the multiprobe resistance formula⁵ to calculate R_H from the scattering coefficients.⁶⁻⁹ A perfect cross with an infinite square-well potential (“hard walls”) quenches only for very specific values of the Fermi energy E_F ,⁷ contrary to experimental results,² which quench for a wide range of E_F . A similar model with a parabolic potential obtains ranges of E_F where realistic-looking quenches occur. For more than two subbands, however, the quench has almost disappeared, whereas early devices^{1,2} probably had between three and nine subbands populated when quenching was observed.

New theoretical work⁹ obtains generic quenching over wide ranges of E_F and width by modifying the geometry and by energy averaging. The important change incorporated into the new model is collimation of the electrons as they enter the cross region. This is accomplished by adiabatic widening of the wire near the junction. Because the widening of the wire is gradual, the electrons

at the Fermi surface do not populate the extra subbands available in the wider region, and because the subbands are depressed in the wider region, the ratio of the longitudinal momentum to the transverse momentum increases: The electrons are collimated.¹⁰ Near zero magnetic field, these collimated electrons are preferentially transmitted straight through the junction, and the Hall voltage is quenched.

The devices used for this experiment were fabricated using a standard method.¹¹ A high-mobility GaAs-Al_x-Ga_{1-x}As heterostructure with a 300-Å cap layer was patterned using electron-beam lithography and reactive-ion etching to remove selectively the cap layer around the edges of the conducting channels. The whole device was then covered with a NiCr/Au gate [(50 Å)/(400 Å)]. The etched regions confine the 2D electron gas to the unetched channels, and the gate above has two effects: Decreasing the gate voltage V_g decreases the channel width (due to the close proximity of the gate at the sides of the channel) and lowers the carrier concentration. No effects of the magnetic nature of the NiCr have been detected, even in ring samples made at the same time, which show Aharonov-Bohm oscillations with peak-to-valley ratios up to ~ 3 at $T=25$ mK.¹² These results also give us confidence that the etching procedure does not degrade the two-dimensional electron gas significantly, despite the absence of conduction in these narrow devices at $V_g=0$ due to edge depletion. $V_g > V_{g\text{thres}} \approx +0.35$ V is required to turn them on (this value varied somewhat each time the device was cooled down). All the samples were made simultaneously on the same wafer, so that there should be little variation between different devices other than that due to the particular geometry.

The measurements were made mainly at $T=4.2$ K, in fields up to ± 5 T using a constant ac current of 10 nA at 11 Hz. The samples investigated each had two cross regions, 6 μm apart and joined by a straight narrow channel of constant width (see top of Fig. 1). One of the two was nominally perfect (radius of curvature of the lithographic corners ~ 400 Å), and the other was one of the following three possibilities: (1) a cross with deli-

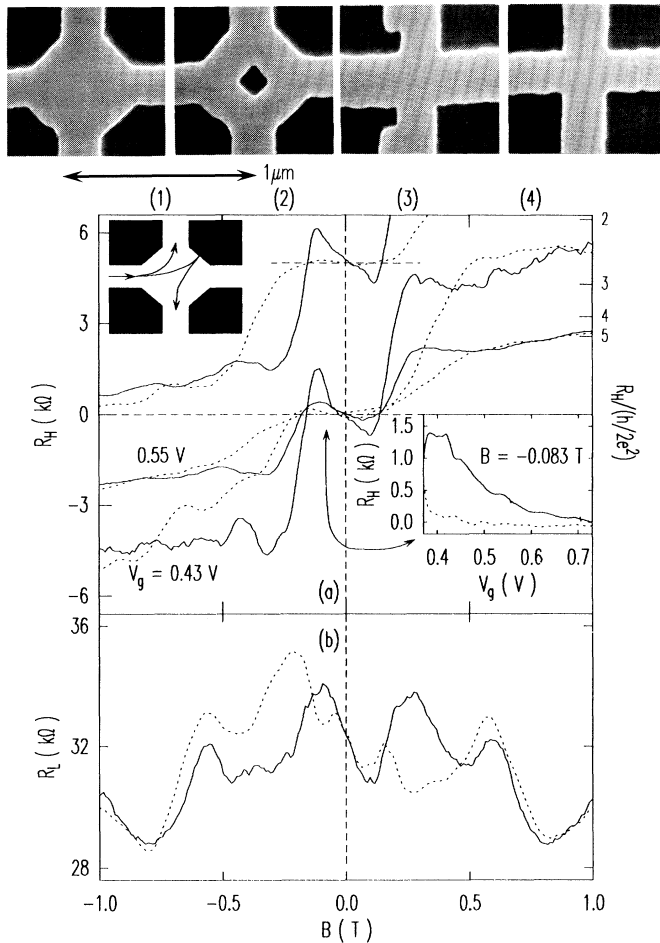


FIG. 1. (Top) Electron micrographs of the following devices: (1) a widened cross, (2) a widened cross with a central dot, (3) a cross with narrow probes, and (4) a "normal" (nominally perfect) cross. (a) R_H vs B for a sample consisting of devices (1) and (4), for several values of V_g . The solid and dotted lines are for the widened and normal crosses, respectively (on the same sample). The trace offset vertically by 5 k Ω shows corresponding results for a different, nominally identical, sample. Inset: A gate-voltage sweep showing that R_H has the wrong sign for all V_g . (b) R_L for $V_g = 0.43$ V, measured on the two sides of the channel. Inset for each figure: The electron paths, as discussed in the text.

berately tapered corners over the last 0.2 μm of each channel; (2) a cross as in (1) but with a diamond-shaped dot in the center, 0.2 μm on a side and leaving an annulus around it ~ 0.25 μm wide; and (3) a cross with voltage probes which were necked down narrower than the current probes (0.25 μm compared with 0.35 μm) to allow them to be pinched off almost completely. For samples (1) and (2), the lithographic linewidths of the channels and probes were 0.29 μm .

The electrical channel widths have been calculated from the positions of Shubnikov-de Haas oscillations

(which are shifted by the one-dimensional confinement).¹³ Fitting the positions by the theory gives widths ranging from ~ 0.19 μm down to ~ 0.09 μm for V_g in the range 0.75 to 0.43 V, for sample (1). The corresponding carrier concentrations n_s are 4.2×10^{15} and $1.2 \times 10^{15}/\text{m}^2$ (from high-field sweeps of R_H). The mobility is estimated to be close to that in the unpatterned material, namely 30 m^2/Vs at high V_g down to ~ 20 m^2/Vs . The number N of (spin-degenerate) subbands occupied is probably between 8 and 2, from counting Shubnikov-de Haas oscillations. The phase-coherence length L_ϕ is expected to be of the order of 1 μm , a little larger than the wide-cross region. The magnetic length scales involved in the problem are the magnetic length $l_B = (\hbar/eB)^{1/2}(2N-1)^{1/2}$, where for large field N is the Landau-level index, and the classical cyclotron radius $r_c = v_F/\omega_c$, where v_F is the Fermi velocity and $\omega_c = eB/m^*$. At $B = 0.1$ T (about where the quenched region ends), $l_B = 0.081$ μm and $r_c = 1.0$ – 0.57 μm , and at $B = 0.4$ T, $l_B = 0.04$ μm and $r_c = 0.26$ – 0.14 μm . The r_c calculated here are for the range of n_s mentioned above, assuming a two-dimensional density of states, which may overestimate r_c by $\lesssim 20\%$ even at small N . It is not clear which length scale is appropriate to the problem, but the collimation may favor r_c .

Figure 1(a) shows the Hall resistance as a function of B for device (1) for two gate voltages. The solid line is for the widened cross, in which R_H is negative in the range of B where the normal cross is quenched. (For all of the devices discussed in this paper, the normal cross exhibited a generic quench, implying little random variation in geometry or dependence on impurity configuration among the devices.) Moreover, the normal cross was quenched for all V_g below a certain value, as evidenced by the gate-voltage sweep shown in the inset in Fig. 1(a), which was performed at $B = -0.083$ T, where (classically) $-130 > R_H > -430$ Ω for $0.75 > V_g > 0.43$ V. To some extent the normal cross develops negative R_H as V_g approaches V_{thres} because the rounded corners in the normal cross are more significant when the channels are very narrow. The fluctuations in $R_H(V_g)$ may result from depopulation of subbands as n_s and channel width decrease, but they certainly do not correspond to a disappearance of the quench at certain voltages, which has been predicted in Refs. 7 and 8. A second, nominally identical device shows the same behavior, as shown offset in Fig. 1(a). The similarity between the two results is so striking that there seems little room for doubt that the effect is due to the particular geometry. The width of the quenched region of B is surprisingly insensitive to V_g . If the quench width increases with n_s and with decreasing w , as found experimentally,¹⁴ then in our case the decrease in n_s may offset that in w . The quenching starts to disappear at $T \gtrsim 10$ K, where the subband energy spacing (a few meV) equals a few $k_B T$. The negative R_H survives to higher T

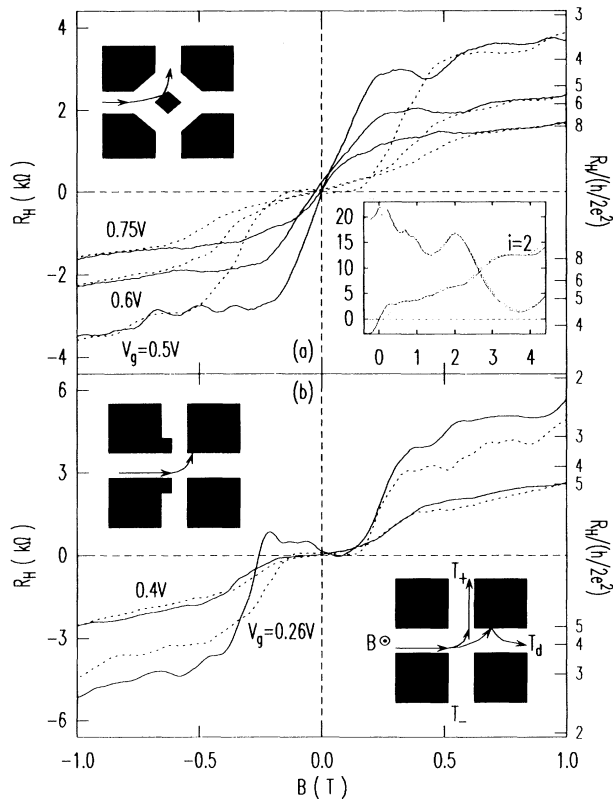


FIG. 2. (a) R_H vs B for various values of V_g . The solid and dotted lines are for the widened cross with a central dot (2) and the normal cross (4) on the same sample. Inset: High-field data which illustrate tracking of the two curves and the usual quantized Hall effect for $V_g = 0.50$ V. (b) R_H vs B for several values of V_g . The solid and dotted lines are for the cross with narrow probes (3) and the normal cross (4) on the same sample.

than the normal quench, flattening off but retaining the same general shape up to 20 K before approaching the classical Hall line.

Figure 1(b) shows the longitudinal resistance R_L for the widened cross sample, measured simultaneously on both sides of the channel, and the structure in R_L lines up with that in R_H . The difference between the traces is due to the difference in Hall voltage at the two junctions, and the resistance measured on one side is the same as that on the other side for the opposite field direction, except where R_H is not antisymmetric. This follows from reciprocity⁵ and fourfold symmetry in the crosses. For $B \gtrsim 1$ T, the resistances R_H and R_L are independent of which probes are used for the measurement [see inset in Fig. 2(a)], which indicates uniformity of n_s over the whole device.

Figure 2(a) displays R_H for three values of V_g for device (2), the widened cross with a dot in the middle. The behavior here is very different: The last plateau matches very well that of the normal cross, but it extends to lower

field, and then the Hall resistance plunges *linearly* to zero at $B=0$. Note that R_H everywhere exceeds the classical value.

Figure 2(b) illustrates the effect of pinched probes [sample (3)]. At high V_g there is very little difference between the two sets of probes, but as the probes get narrower with decreasing V_g , the quenched region widens in the narrower cross relative to the normal cross. The quench also starts to develop negative-going features reminiscent of the widened cross, and some asymmetry. The last plateau for the narrow probes is consistently above that for the normal probes except at very high V_g . These data may be contrasted with the results from Chang and Chang³ who found no quench with similarly notched voltage probes in somewhat wider samples. In the latter case the current-carrying channel was too wide for effective collimation. The data here are not yet good enough to compare with the prediction⁶ that a device with weakly-coupled probes should not show quenching.

We believe the data can be explained qualitatively in the following way: The subband structure in the wire is smoothly connected to that in the cross region, so that electrons entering the cross stay in the same subband and become collimated (provided that the intersubband scattering time is greater than the transit time through the cross). Since the lithography and confinement can never be perfectly sharp, this collimation is bound to occur even in the normal cross where the corners are rounded (lithographically) with a radius of ≈ 400 Å. Semiclassically, collimation corresponds to electron trajectories continuing straight ahead with a small spread. In a normal cross, a finite B is required to bend the trajectories enough to enter the Hall probe on the "correct" side.^{15,16} The radius of curvature must be of the order of the probe width. Electrons that do not bend around enough continue on along the wire and do not contribute to the Hall effect; hence the quenching [see inset in Fig. 2(b)]. Because the entrances to the cross and the voltage probes are widened in sample (1), a larger radius is sufficient to bend the trajectories into the correct probe, so the negative R_H is suppressed by a lower field. In the device with notched probes, the quenched region is wider than in the normal cross, even though the channel width in each is the same. Alternatively, if the current had been fed through the notched probes, the collimation would have been stronger and the quench would still be wide (satisfying reciprocity constraints⁵). The transverse momentum for a particular subband is unaffected by n_s , but the longitudinal momentum increases with n_s , so that the collimation will increase with n_s . The concomitant increase in N , however, will reduce the collimation. If increasing n_s dominates, this should give a better quench, and may explain the widening of the quench region with increasing n_s in wires of constant width.¹⁴

This simple picture of trajectories allows us to understand the behavior of the transmission coefficients that

arise in the quantum-mechanical treatment of the transport through the cross. The Hall resistance is governed by the transmission coefficients, T_+ into the Hall probe favored by the Lorentz force, T_- into the opposite probe, and T_d directly through the cross [see Fig. 2(b)]. In a twofold-symmetric cross with two mirror planes [such as sample (3) if one ignores the widening of the voltage probes away from the cross],⁵

$$R_H = \frac{(h/2e^2)(T_+ - T_-)}{2T_d\hat{T}_d + (T_d + \hat{T}_d)(T_+ + T_-) + T_+^2 + T_-^2},$$

where the \hat{T}_d describes direct transmission between the voltage probes (and $\hat{T}_d \equiv T_d$ for fourfold symmetry⁷⁻⁹). At $B=0$, $T_+ = T_-$, and as B increases, T_d decreases. The quenching results from the dominance of T_d or the near cancellation of T_+ and T_- .^{9,15} In the widened cross, T_- exceeds T_+ because of trajectories reflected from the diagonal wall into the "wrong" probe [see inset in Fig. 1(a)]. In the widened cross with the hole, T_d is suppressed so that $T_+ > T_- \gg T_d$; hence R_H is enhanced over the classical value. The formula above is strictly antisymmetric under field reversal, so the asymmetry seen in Fig. 2(b) arises from a lack of twofold symmetry, either due to imperfect lithography or to impurities.

The last plateau probably appears in all samples when edge states start to form, suppressing T_- . T_d and \hat{T}_d are also suppressed with increasing field, but in the region of the last plateau, they are still nonzero due to scattering between edge states entering and leaving the current and voltage probes. We stress that, in contrast to low fields, T_d and \hat{T}_d are nonzero not because of direct transmission through the center of the cross but via the scattering process just described. This explains the equivalence of the last plateau of the geometries (1), (2), and (4). Ignoring T_- , one may write $R_H \approx (h/2e^2)/(T_+ + T_d + \hat{T}_d)$. Because T_d and T_- are not strictly zero (as they would be for the quantized Hall effect), the plateaus do not lie precisely at integers. As B increases, T_d decreases by one channel at a time as each edge state in turn becomes narrow enough to prevent exchange between the two sides, and so R_H rises in a series of steps to the "real" last plateau. Such intermediate plateaus can be seen in Fig. 2 and have also been predicted.^{8,7} The higher plateau in the cross with pinched probes can be explained by assuming that \hat{T}_d (transmission between the pinched probes) is smaller than T_d , while the sum $T_+ + T_d$ is approximately the number of channels in the wide probe. (In the quantized Hall

effect, these approximations become exactly true:⁵ viz., $T_+ + T_d \equiv N$ and $\hat{T}_d \equiv 0$.) It is the reduction of \hat{T}_d which gives rise to the enhancement of the last plateau of the cross with two pinched probes.

In conclusion, we have found that different cross geometries can make R_H quenched, enhanced, or even negative. The quenching and the last plateau do not seem intimately related, as the plateau is seen even when R_H is enhanced instead of quenched. We attribute the effects to geometrical scattering of the electrons entering the cross region. The last plateau results from edge states as in the quantized Hall effect, but the lack of exact quantization reflects the incomplete suppression of T_d .

We gratefully acknowledge the advice on the channel isolation method given by K. Y. Lee and A. B. Fowler, and on lithography by S. Rishton and D. P. Kern. We also thank J. Stasiak for the loan of equipment, and M. Berger, D. Lacey, K. Milkove, N. Penebre, and S. Wieland for technical assistance.

¹M. L. Roukes, A. Scherer, S. J. Allen, Jr., H. G. Craighead, R. M. Ruthen, E. D. Beebe, and J. P. Harbison, Phys. Rev. Lett. **59**, 3011 (1987).

²C. J. B. Ford, T. J. Thornton, R. Newbury, M. Pepper, H. Ahmed, D. C. Peacock, D. A. Ritchie, J. E. F. Frost, and G. A. C. Jones, Phys. Rev. B **38**, 8518 (1988).

³A. M. Chang and T. Y. Chang (to be published).

⁴C. W. J. Beenakker and H. van Houten, Phys. Rev. Lett. **60**, 2406 (1988).

⁵M. Büttiker, Phys. Rev. Lett. **57**, 1761 (1986); Phys. Rev. B **38**, 9375 (1988).

⁶F. M. Peeters, Phys. Rev. Lett. **61**, 589 (1988).

⁷D. G. Ravenhall, H. W. Wyld, and R. L. Schult, Phys. Rev. Lett. **62**, 1780 (1989).

⁸G. Kirczenow, Phys. Rev. Lett. **62**, 1970 (1989); (unpublished).

⁹H. U. Baranger and A. D. Stone (to be published).

¹⁰C. W. J. Beenakker and H. van Houten (unpublished).

¹¹T. P. Smith, III, H. Arnot, J. M. Hong, C. M. Knoedler, S. E. Laux, and H. Schmid, Phys. Rev. Lett. **59**, 2802 (1987).

¹²C. J. B. Ford *et al.* (to be published).

¹³K.-F. Berggren, G. Roos, and H. van Houten, Phys. Rev. B **37**, 10118 (1988).

¹⁴M. L. Roukes *et al.* (unpublished).

¹⁵Y. Takagaki, K. Gamo, S. Namba, S. Ishida, S. Takaoka, K. Murase, K. Ishibashi, and Y. Aoyagi, Solid State Commun. **68**, 1051 (1988). From the results of this experiment, one sees that, at least at low field, $T_d^2 > T_+ T_-$.

¹⁶Y. Avishai and Y. B. Band (unpublished).

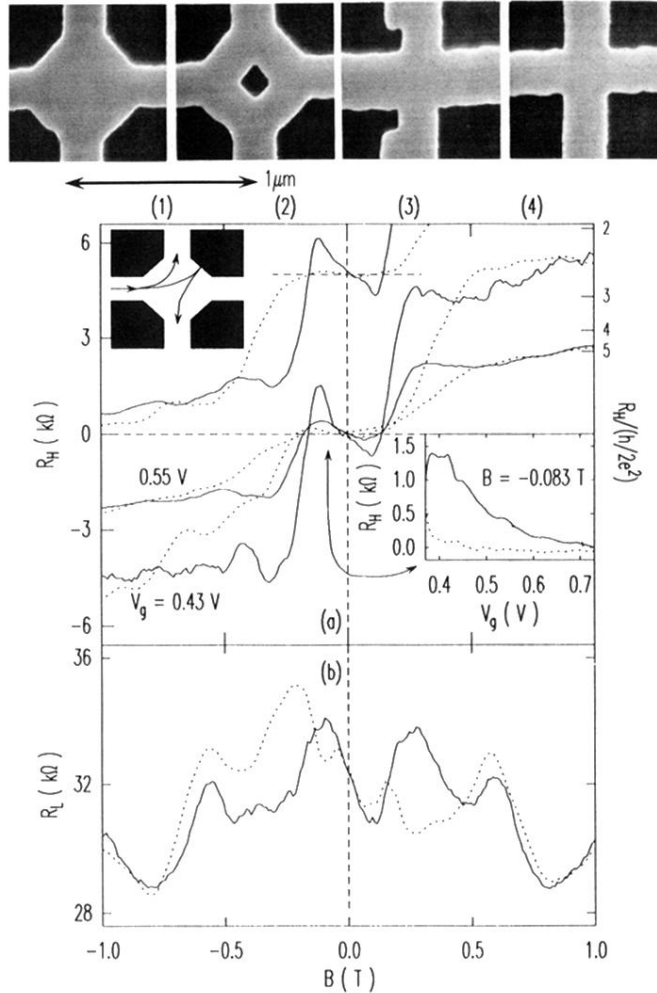


FIG. 1. (Top) Electron micrographs of the following devices: (1) a widened cross, (2) a widened cross with a central dot, (3) a cross with narrow probes, and (4) a “normal” (nominally perfect) cross. (a) R_H vs B for a sample consisting of devices (1) and (4), for several values of V_g . The solid and dotted lines are for the widened and normal crosses, respectively (on the same sample). The trace offset vertically by $5 \text{ k}\Omega$ shows corresponding results for a different, nominally identical, sample. Inset: A gate-voltage sweep showing that R_H has the wrong sign for all V_g . (b) R_L for $V_g = 0.43 \text{ V}$, measured on the two sides of the channel. Inset for each figure: The electron paths, as discussed in the text.